Advanced Composite Materials, 2014
Vol. 23, No. 3, 261–273, http://dx.doi.org/10.1080/09243046.2013.851357

Simple electric-voltage-change-analysis method for delamination of thin CFRP laminates using anisotropic electric potential function

Akira Todoroki[a]* and Masahiro Arai[b]

[a]*Department of Mechanical Sciences and Engineering, Tokyo Institute of Technology, 2-12-1 Ookayama, Meguro (i1-58), Japan;* [b]*Department of Mechanical System engineering, Shinshu University, 4-17-1 Wakasato, Nagano-city, Nagano, Japan*

(*Received 28 March 2013; accepted 25 September 2013*)

Although the electrical-resistance-change method is useful for monitoring delamination cracking of carbon-fiber-reinforced plastic (CFRP) laminates, the method requires many experiments or FEM analyses to obtain the relationship between the electrical resistance changes and parameters describing delamination cracking. In our previous studies, one of the authors proposed using an anisotropic electric potential function to analyze electric current density in CFRP laminates. The function was applied only to thick CFRP laminates. In the present study, the method is expanded to thin CFRP laminates using an image method. The number of images is determined using the electric current analysis of thick CFRP laminates. The electric potential changes caused by delamination cracking can be calculated using an anisotropic doublet line. The associated method is applied to calculate the electric voltage change at the surface of a thin CFRP laminate. The results are compared with an FEM analysis, and, overall, the method is shown to be very effective.

Keywords: delamination; electric current; analysis; potential flow; doublet

1. Introduction

Carbon-fiber-reinforced plastic (CFRP) composites have high electric conductance in the fiber direction, but very low electric conductance in the transverse direction; such composites have strongly orthotropic materials from the point of view of electric conductance.[1–7] In a ply of unidirectional CFRP, the electric conductance in the transverse direction is aided by carbon fiber contact as well as conductance in the thickness direction but the conductance is small in both the transverse and thickness direction. If a resin-rich layer exists between the plies, conductance in the thickness direction falls below that of the transverse direction.[4]

A method to monitor delamination crack in a CFRP laminate was proposed by Todoroki [7]: multiple electrodes are mounted on the CFRP laminate and changes in the electrical resistance between the electrodes are measured. This method requires the development of the relationship between electrical-resistance changes and delamination cracking parameters, so that location and size of the delamination can be monitored. If statistical response surfaces are adopted to uncover this relationship, many experiments are necessary but nevertheless costly. To reduce costs, a simple analytical method is required. However, one that calculates the electrical potential changes in CFRP

*Corresponding author. Email: atodorok@ginza.me.stitech.ac.jp

laminates is not suitable because of the strongly anisotropic electrical conductance of CFRPs. With the lack of an analytical method, a numeric analysis requires a very fine mesh in the thickness direction of a CFRP laminate. This introduces high computational cost, and thus impedes any practical application of the electrical-resistance-change method.

To determine the electric current flow of the strongly anisotropic CFRP laminates, Todoroki [5] has proposed a new anisotropic electric potential function; the electric current density of each ply was analyzed for a thick unidirectional CFRP and a thick cross-ply CFRP laminate. Using this potential function, a new lamination theory to calculate the electric conductance of a thick CFRP laminate was developed and its effectiveness was demonstrated.[6]

In the present study, the anisotropic electric potential function method is revised to treat thin unidirectional CFRP laminates. An image analysis method, which is usually used for the potential flow analysis of perfect fluid flows, is adapted for anisotropic CFRP laminates. The results are compared with FEM-based results; the applicability of the image analysis in this different context is also investigated here. On the basis of the improved method, a new anisotropic doublet analysis method is proposed to calculate the electrical voltage changes caused by a delamination crack. This anisotropic doublet method is applied to a CFRP beam with a delamination crack, and the surface electric potential is compared with FEM-based results.

2. Analytical method

2.1. Anisotropic electric potential function analysis

In this section, the anisotropic electric potential function proposed in previous papers [5, 6] is briefly described. Let us consider a unidirectional CFRP laminate composed of a homogenous orthotropic material; a Cartesian coordinate system is setup so that the fiber direction lies in the x-direction, the in-plane transverse direction is in the y-direction, and the thickness direction is in the z-direction. Introducing the electric potential ϕ, the electric current density i_x, i_y, and i_z is defined as

$$i_x = -\sigma_x \frac{\partial \phi}{\partial x}, \quad i_y = -\sigma_y \frac{\partial \phi}{\partial y}, \quad i_z = -\sigma_z \frac{\partial \phi}{\partial z}, \tag{1}$$

where σ_x, σ_y, and σ_z are the electric conductivities in each direction. For a CFRP laminate, the resin-rich interlamina is neglected and the CFRP laminate is assumed to have uniform electric conductance in the thickness direction. With no electric current input, the equation for the continuity of the electric current is

$$\frac{\partial}{\partial x}(i_x) + \frac{\partial}{\partial y}(i_y) + \frac{\partial}{\partial z}(i_z) = 0. \tag{2}$$

Substitution of Equation (1) into Equation (2) gives

$$\sigma_x \frac{\partial^2 \phi}{\partial x^2} + \sigma_y \frac{\partial^2 \phi}{\partial y^2} + \sigma_z \frac{\partial^2 \phi}{\partial z^2} = 0. \tag{3}$$

Let us consider a two-dimensional case of a CFRP plate set in the x-z plane (corresponding to fiber and thickness directions). To deal with the orthotropic coordinate, affine coordinates are adopted

$$\xi = \frac{x}{\sqrt{\sigma_x}}, \quad \eta = \frac{z}{\sqrt{\sigma_z}}, \tag{4}$$

by which Equation (3) then becomes

$$\frac{\partial^2 \phi}{\partial \xi^2} + \frac{\partial^2 \phi}{\partial \eta^2} = 0. \tag{5}$$

Equation (5) is the isotropic Laplace equation, which is similar to the velocity potential of a perfect fluid.

Let us consider that, on the same surface of this CFRP plate, a source-sink couple of electric current is located; for definiteness, the source is set at $(-a, 0)$ and the sink at $(a, 0)$, where $a > 0$ (see Figure 1). Using the potential flow for this source-sink couple, the electric current density can be formulated as

$$\begin{aligned} i_x &= \frac{I}{\pi\sqrt{\sigma_x \sigma_z}} \left\{ \frac{x+a}{\dfrac{(x+a)^2}{\sigma_x} + \dfrac{z^2}{\sigma_z}} - \frac{x-a}{\dfrac{(x-a)^2}{\sigma_x} + \dfrac{z^2}{\sigma_z}} \right\} \\ i_z &= \frac{I}{\pi\sqrt{\sigma_x \sigma_z}} \left\{ \frac{z}{\dfrac{(x+a)^2}{\sigma_x} + \dfrac{z^2}{\sigma_z}} - \frac{z}{\dfrac{(x-a)^2}{\sigma_x} + \dfrac{z^2}{\sigma_z}} \right\} \end{aligned} . \tag{6}$$

For a thin CFRP laminate, the electric potential is uniform in the thickness direction. The electric current density can be easily obtained using the conventional lamination theory for electric conductance with uniform electric potential.[6] For a thick CFRP, however, the electric potential distribution is non-uniform, thus the thin CFRP lamination theory is inapplicable for calculating the electric conductance of the CFRP laminate. For a thick CFRP laminate, the form of the non-uniform electric potential is assumed to be similar to the unidirectional thick CFRP. The contribution of each ply is obtained using the effective cross-sectional area, and the electric current density is obtained using the contribution function. If angle plies are included in the CFRP laminate, a couple of + 45° and −45° plies are combined as a coupled-double-thickness single ply. Details of these aspects have been presented in a previous paper.[6]

The analysis is restricted to a thick CFRP in which the electric current density of the bottom ply is almost zero. In our previous paper, the integration along the thickness direction of the electric current density on the mid-plane ($x = 0$) between the electrodes was

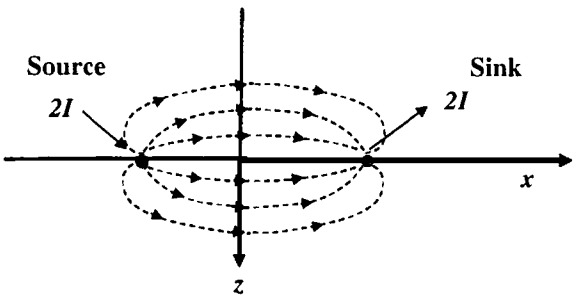

Figure 1. Source and sink model considered here.

given, and the integrated value normalized by the applied electric current. This enables us to quantify the thickness of the CFRP laminate. The normalized integral value δ_t is

$$\delta_t = \frac{1}{I}\int_0^t i_x(0,z)dz = \frac{2}{\pi}\tan^{-1}\left(\frac{t}{a\lambda}\right), \tag{7}$$

where t is the thickness of the laminate, $2a$ the electrode spacing, and λ the square root of the conductance ratio ($\lambda = \sqrt{(\sigma_z/\sigma_x)}$). In the previous study, a thick CFRP is defined as a laminate for which 90% of the total electric current conducts within a thickness t. This leads to a thickness criterion obtained by rearranging Equation (7) with $\delta_t = 0.9$ yielding condition

$$t \geq 6.3a\lambda. \tag{8}$$

2.2. *Analysis of thin CFRP using image analysis*

In actual CFRP laminated structures, not only thick CFRP laminates but also thin CFRP laminates are used. Thin fabric CFRPs are used in automobile panels. For a thin fabric CFRP, the laminate has isotropic properties in the plane but a different electric conductance in the thickness direction; hence, in this instance, electric current analysis is important in understanding the characteristics of actual CFRP products.

In the ξ-η coordinate system, the anisotropic electric potential function becomes isotropic. This implies that in performing an electric current density analysis of a thin CFRP laminate, an infinite number of images can be positioned in the plane.

Figure 2 shows the x-z cross-sectional view for a couple of electrodes placed on the top surface of a thin CFRP laminate of thickness t. An electric current source is shown as a filled dot and a sink ground electrode is shown as an open dot. The origin of the coordinate system is mid-point between the electrodes. If the CFRP laminate is sufficiently thick that Equation (8) applies, the electric current density can then be obtained using Equation (6). If the CFRP laminate does not satisfy Equation (6), the electric current density must be calculated with the placement of source and sink images as appropriate for a finite thickness CFRP. The schematic representation of the images of sources and sinks is shown in Figure 3. In the present study, the image is limited to z-direction because the thickness is the most important issue here. The cross-sectional view given in Figure 2 is identical to the bottom half of the part of thickness $2t$ in the area for $N = 0$ in Figure 3. In this figure, N denotes the number of sets of plus and minus images. For example, $N = 10$ includes the image from #−10 to #10.

In Figure 3, an electric current source-sink couple has been placed on the line $z = 0$ in the area for $N = 0$. In the image of #1, a source-sink couple has been placed on the line for $z = 2t$. In general, a source-sink couple is placed on the line $z = 2nt$ in the image for #n. Source-sink couples of an image must simultaneously be placed at

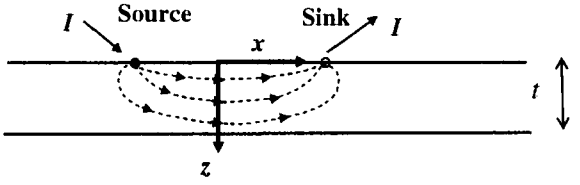

Figure 2. Electric current model using a couple of a source and a sink for thin CFRP.

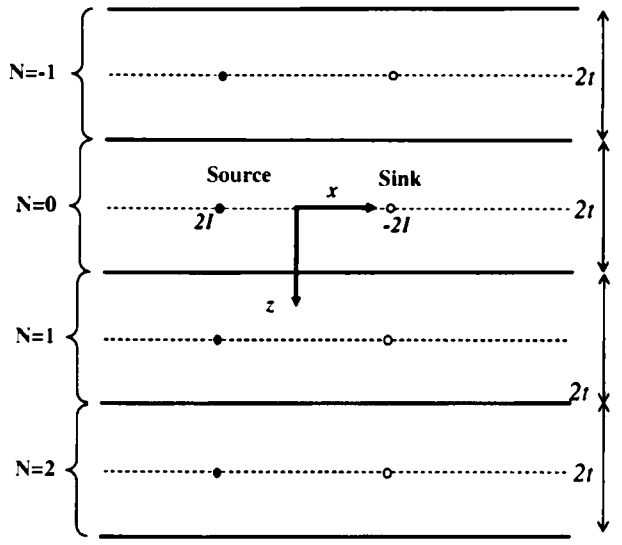

Figure 3. Schematic representation of image method for electric current of a thin CFRP laminate.

reflected locations. For the image of #−1, the location is $z = -2t$, whereas for the image of #−n, $z = -2nt$. The electric current densities i_x and i_z from the image of #n is given as follows:

$$i_x = \frac{I}{\pi\sqrt{\sigma_x\sigma_z}}\left\{\frac{x+a}{\frac{(x+a)^2}{\sigma_x}+\frac{(z-2tn)^2}{\sigma_z}} - \frac{x-a}{\frac{(x-a)^2}{\sigma_x}+\frac{(z-2tn)^2}{\sigma_z}}\right\}$$
$$i_z = \frac{I}{\pi\sqrt{\sigma_x\sigma_z}}\left\{\frac{z-2tn}{\frac{(x+a)^2}{\sigma_x}+\frac{(z-2tn)^2}{\sigma_z}} - \frac{z-2tn}{\frac{(x-a)^2}{\sigma_x}+\frac{(z-2tn)^2}{\sigma_z}}\right\} \quad (9)$$

If n sets of images are required, the electric current density is obtained by summing up the electric current densities from the image of #−n to that of #n:

$$i_x = \sum_{k=-n}^{n}\frac{I}{\pi\sqrt{\sigma_x\sigma_z}}\left\{\frac{x+a}{\frac{(x+a)^2}{\sigma_x}+\frac{(z-2tk)^2}{\sigma_z}} - \frac{x-a}{\frac{(x-a)^2}{\sigma_x}+\frac{(z-2tk)^2}{\sigma_z}}\right\}$$
$$i_z = \sum_{k=-n}^{n}\frac{I}{\pi\sqrt{\sigma_x\sigma_z}}\left\{\frac{z-2tk}{\frac{(x+a)^2}{\sigma_x}+\frac{(z-2tk)^2}{\sigma_z}} - \frac{z-2tk}{\frac{(x-a)^2}{\sigma_x}+\frac{(z-2tk)^2}{\sigma_z}}\right\} \quad (10)$$

The appropriate number of images can be determined using Equation (8). The electric current in the region from $z = 0$ to $z = t$ (the target area of the thin CFRP laminate) of the image is very small when a source-sink couple of an image is located far from the target area.

The condition that the contribution to the electric current density from the image of $\#n$ at $z = 0$ is small is similar to the condition defining a thick CFRP, i.e. Equation (8). To improve accuracy compared with the condition of the thick CFRP, δ_t is set here to 0.99 (=99%). The condition obtained is

$$N \geq 63.7\frac{a\lambda}{2t}. \tag{11}$$

Using Equation (11), the N required to obtain accurate electric current density for a thin CFRP laminate can now be obtained.

2.3. *Analysis of delamination using an anisotropic doublet line*

In fluid dynamics, if a plate is placed in a uniform flow, the velocity potential of the perfect flow can be obtained using the Joukowski transformation. Simple analyses of airfoils can be performed using three cases: distributed source, distributed doublet comprising a source and a sink, and distributed vortex.[8] As the electric potential function is isotropic for the ξ-η coordinate, the velocity potential of the perfect flow can be applied to the electric current flow in the CFRP laminate.

A plate in a flow field can be produced using the placement of a distributed flow that annihilates flow perpendicular to the plate. The plate in the flow corresponds to a crack in the electric current flow. To annihilate the electric current perpendicular to the crack plane, a distributed doublet must be placed on the crack surface. In the present study, a single delamination crack is considered.

Using the illustration of Figure 4, consider a delamination crack located between $(x_1,0)$ and $(x_2,0)$; $z = 0$ is not the surface but is here moved parallel to the crack location. To annihilate the electric current flow perpendicular to the crack, a distributed double flow that has flow perpendicular to the x-coordinate must be placed on the crack, as shown in Figure 4.

If a doublet of strength μ is placed at the origin of the isotropic ξ-η coordinate, the perfect fluid velocity potential of a doublet, having flow in the η direction, can be expressed as

$$\phi = \frac{\mu \sin\theta}{2\pi r}. \tag{12}$$

where r and θ determine a polar coordinate system with origin at the center of the doublet. A transformation of Equation (12) into the ξ-η coordinate gives

$$\phi = \frac{\mu \sin\theta}{2\pi r} = \frac{\mu \eta}{2\pi r^2} = \frac{\mu \eta}{2\pi(\xi^2 + \eta^2)} \tag{13}$$

As shown in our previous paper,[5] the electric current densities in the ξ-direction, i_ξ, and η-direction, i_η, are

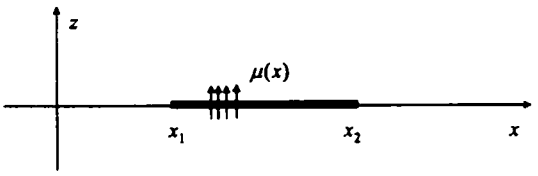

Figure 4. Schematic representation of doublet distribution model.

$$\begin{aligned} i_\xi &= -\sqrt{\sigma_x \sigma_z}\frac{\partial \phi}{\partial \xi} \\ i_\eta &= -\sqrt{\sigma_x \sigma_z}\frac{\partial \phi}{\partial \eta} \end{aligned} \tag{14}$$

From Equation (13),

$$\begin{aligned} \frac{\partial \phi}{\partial \xi} &= -\frac{\mu}{2\pi}\frac{\xi\eta}{(\xi^2+\eta^2)^2} \\ \frac{\partial \phi}{\partial \eta} &= \frac{\mu}{2\pi}\frac{\xi^2-\eta^2}{(\xi^2+\eta^2)^2} \end{aligned} \tag{15}$$

Combining Equations (14) and (15) gives

$$\begin{aligned} i_x &= \frac{i_\xi}{\sqrt{\sigma_z}} = \frac{\mu\sqrt{\sigma_x}}{2\pi}\frac{\left(\frac{x}{\sqrt{\sigma_x}}\right)\left(\frac{z}{\sqrt{\sigma_z}}\right)}{\left\{\left(\frac{x}{\sqrt{\sigma_x}}\right)^2+\left(\frac{z}{\sqrt{\sigma_z}}\right)^2\right\}^2} \\ i_z &= \frac{i_\eta}{\sqrt{\sigma_x}} = -\frac{\mu\sqrt{\sigma_z}}{2\pi}\frac{\left(\frac{x}{\sqrt{\sigma_x}}\right)^2-\left(\frac{z}{\sqrt{\sigma_z}}\right)^2}{\left\{\left(\frac{x}{\sqrt{\sigma_x}}\right)^2+\left(\frac{z}{\sqrt{\sigma_z}}\right)^2\right\}^2} \end{aligned} \tag{16}$$

To annihilate the electric current perpendicular to the crack surface, a distribution of the strength of $\mu(x)$ is placed on the crack surface. To determine the strength distribution $\mu(x)$, the integral equation must be solved so that annihilation of the electric current is achieved.

Let $i_z(x,z)$ is the electric current density by the source-and sink, $i_{z,\text{crack}}(x,z)$ is the electric current density by a crack (the real delamination crack is considered here because of simplicity), and d is the depth of the delamination crack from the surface.

$$i_{z,\text{crack}}(x,z) = -\frac{\sqrt{\sigma_z}}{2\pi}\int_{x1}^{x2}\mu(s)\frac{\left(\frac{x-s}{\sqrt{\sigma_x}}\right)^2-\left(\frac{z-d}{\sqrt{\sigma_z}}\right)^2}{\left\{\left(\frac{x-s}{\sqrt{\sigma_x}}\right)^2+\left(\frac{z-d}{\sqrt{\sigma_z}}\right)^2\right\}^2}ds, \tag{17}$$

The integral equation is given as follows.

$$i_z(x,d) + i_{z,\text{crack}}(x,d) = 0 \tag{18}$$

As shown in Figure 4, the z-coordinate is moved parallel to the doublet center. The translation implies setting $z = d$ in Equation (17) giving

$$i_z(x,0) - \frac{\sigma_x\sqrt{\sigma_z}}{2\pi}\int_{x1}^{x2}\frac{\mu(s)}{(x-s)^2}ds = 0 \tag{19}$$

Equation (19) is a hyper-singular integral equation. An analytical solution has been given [9], but is written in integral form and is thus not easy to use. A numerical solution to Equation (19) has been given [10, 11]. Thus, after obtaining the doublet distribution $\mu(x)$, the electric voltage change caused by the delamination crack can be calculated from Equation (13);

$$V(x,z) = 2\{\phi(x,z) - \phi_0(x,z)\} = -\frac{1}{\pi}\int_{x1}^{x2}\mu(s)\frac{\left(\frac{z}{\sqrt{\sigma_z}}\right)}{\left(\frac{x-s}{\sqrt{\sigma_x}}\right)^2+\left(\frac{z}{\sqrt{\sigma_z}}\right)^2}ds \tag{20}$$

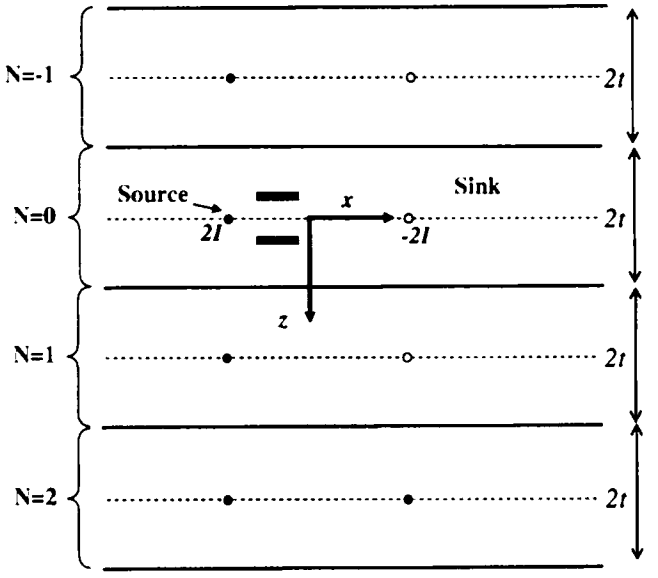

Figure 5. Schematic representation of image method for doublet model analysis.

where ϕ_0 is the electric potential before delamination cracking. The electric potential ϕ is doubled because we have the real delamination crack and image delamination crack of $N = 0$.

It is not easy to deal with the image analysis of the distributed doublet for a thin CFRP laminate. To solve the exact image analysis of the double, the doublet should be distributed at every image and many simultaneous hyper-singular integral equations must be solved.

As the electric conductance of the thickness direction of a CFRP laminate is very small compared with that of the fiber direction, the electric current flows in the thickness direction are generally small. For example, the electric conductance σ_z is approximately of order 10^{-2}–10^{-7} compared with the electric conductance in the fiber direction σ_0. The affine transformation of Equation (4) indicates that the delamination is far from the surface in the η-coordinate even if the delamination crack is located near the surface of the actual coordinate. Figure 5 shows a schematic representation of the approximated image analysis for the doublet analysis. Only the image doublet of $N = 0$ is included here; this means the results of Equation (19) should be doubled, and the effect is very important. Even for thin CFRPs of 1-mm thickness, the image of $N = 1$ has the effect of a delamination crack located more than 10 mm away; this means the effect is very small. Therefore, to simplify the analytical method, only the doublet image of $N = 0$ is considered here. Although the simplification gives a small computational error, the method provides a significantly simpler analysis.

3. Results and discussion

3.1. Analysis target

The new analytical method using the distributed anisotropic doublet is applied to an actual delamination crack of a thin unidirectional CFRP. Figure 6 shows a CFRP beam used for the analysis. The length of the beam is 60 mm; its thickness is 3 mm. The

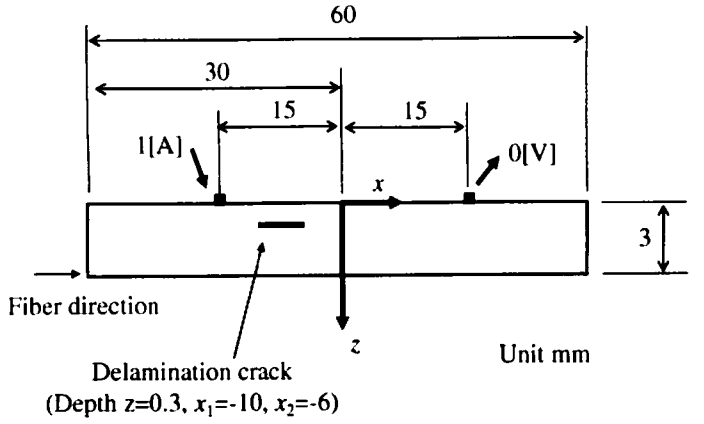

Figure 6. Specimen configurations.

stacking sequence of the thin CFRP beam is unidirectional: the fiber direction is the specimen's longitudinal direction. The origin of the x-z coordinate system is set at the center of the specimen's top surface; the origin of the z-axis is located on the CFRP beam surface here. At the point $(x, z) = (-15, 0)$, a direct current of 1 A is applied, whereas a grounded (0 V) electrode is placed at $(x, z) = (15, 0)$. For the FEM analysis, the commercially available ANSYS ver.11.0 is adopted. Each of the 72,000 elements for the mesh is square of length 0.05 mm. As the ratio of the electric conductivity is important for the electric current analysis, σ_x is set to 1 S/m, and σ_z is set to 0.01 S/m. This conductance ratio is approximately the same as that of Ref. [3]

There is no delamination crack in the image analysis model to confirm the applicability of the new image analysis. To verify the applicability of the new image analysis, two kinds of models are adopted here. The first has a delamination crack 4 mm in length with a depth of 0.3 mm. The delamination crack tips are located at $x_1 = (-10, 0.3)$ and $x_2 = (-6, 0.3)$. To investigate the influence of delamination depth, the second has a delamination crack of 8 mm length with depth 1.0 mm. The delamination crack tips are situated at $x_1 = (-10, 1)$ and $x_2 = (-2, 1)$. For the FEM calculations, the nodes are doubly defined at the crack surface, and the delamination crack surfaces are electrically insulated from each other.

3.2. Results of thin CFRP

To investigate the performance of the image model for a thin CFRP, the electric current density of a thin CFRP beam without a delamination crack is analyzed here, and the results are compared with the FEM results.

Figure 7 shows the electric current density i_x at cross-section $x = 0$; the ordinate is i_x (A/mm^2) and the abscissa gives depth z (mm). The solid curve represents the FEM result and the open circles are the analytical results obtained using the image analysis. As shown in Fig.7, the image analysis provides excellent results for the electric current density.

Figure 8 shows the electric current density i_z at the depth of 0.3 mm. The ordinate gives i_z (A/m^2) and the abscissa represents the x-direction at $z = 0.3$ mm. (In the following sub-section, a delamination crack will be made on this line segment from

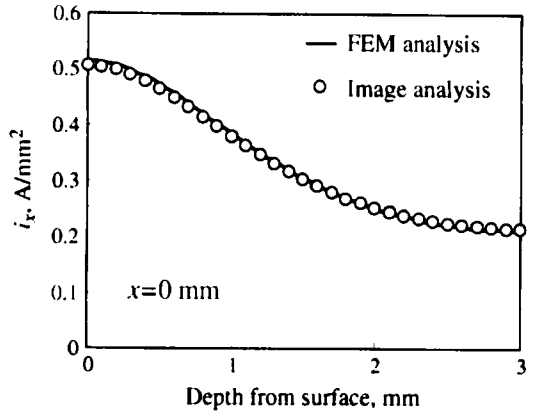

Figure 7. Electric current density of x-direction at $x = 0$.

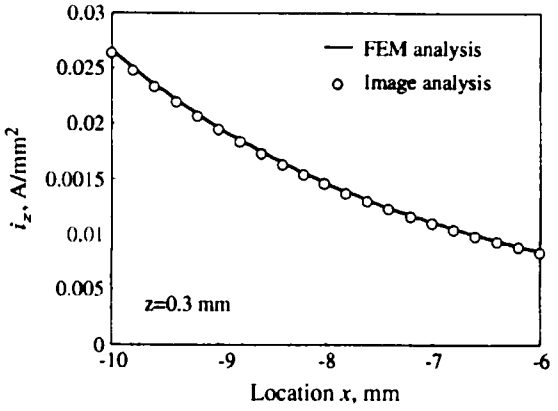

Figure 8. Electric current density of z-direction at $z = 0.3$ [mm].

$x = -10$ mm to $x = -6$ mm.) The solid curve presents results from the FEM analysis and the open circles those from image analysis. Clearly, the image analysis gives an excellent estimation of the thin CFRP. Note that although the required least number of sets is $N = 16$, obtained using Equation (11), $N = 20$ is used here to obtain exact results.

3.3. *Surface voltage change caused by delamination*

The surface electric voltage change is calculated for a CFRP beam with a 4-mm length delamination crack at a depth of $z = 0.3$ mm.

To solve the hyper-singular integral equation, Equation (19), a boundary element method is adopted that uses a solution corresponding to a uniform potential slope to cancel the singularity; the method is described in detail in Refs. [10, 11] For the boundary element analysis, singular elements were chosen at the delamination crack tip. In particular, the delamination crack is divided into 16 elements (17 nodes). In brief, using the method, a distributed doublet $\mu(x)$ is obtained.

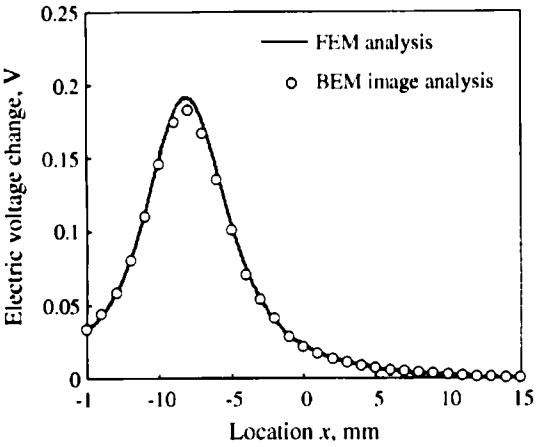

Figure 9. Electric voltage change calculated using the doublet distribution BEM method. (Delamination crack z = 0.3 [mm], x_1 = −10 [mm], x_2 = −6 [mm]).

With $\mu(x)$, the electric voltage change at the top surface $z = 0$ from $x = 15$ mm to $x = -15$ mm is calculated using Equation (20). Figure 9 shows the results of the doublet analysis: the ordinate gives the electric voltage change from the electric potential without a delamination crack, and the abscissa gives the x-coordinate between the electrodes. The solid curve represents the results of the FEM analysis and the open circles are the results of the distributed doublet analysis. As mentioned in the previous section, the only two images of the distributed doublet of $N = 0$ are counted; the other images are neglected for this calculation to simplify the analysis. Although there is small computational error, the results of the distributed doublet show excellent agreement with the FEM results.

To avoid solving the hyper-singular integral equation directly, several other methods are available besides the boundary element analysis. One of the simplest methods is a small-parallel-shift method of z-axis from $z = 0$ in Equation (17). With a small non-zero value substituted for z in Equation (17), a hyper-singularity is prevented from forming at the delamination crack tips. In the present study, a value $z = 0.01$ enables us to consider the uniform strength of the doublet in each small segment. To calculate the distributed doublet, the delamination crack is divided into eight segments that have uniform doublet strength within the each segment. Instead of solving the hyper-singular integral equation, eight simultaneous linear equations in the eight unknown doublet strengths are solved. The analysis can be done with spreadsheet software without using complicated programming. Figure 10 shows the results of this simple analysis. The results agree very well with the FEM results. The simple method depends on the adequateness of the small value. The value used here might not always be the best value.

Figure 11 shows the results of larger delamination at a deeper z-location: length is 8 mm and depth is $z = 1.0$ mm. The delamination crack tips are located at $x_1 = -10$ mm and $x_2 = -2$ mm. The ordinate gives the difference from the electric voltage of the thin CFRP without a delamination crack, and the abscissa gives the x-location. The solid curve presents the results of FEM and the open triangles indicate the results of the analysis in which a small parallel shift was used. The open circles indicate the results

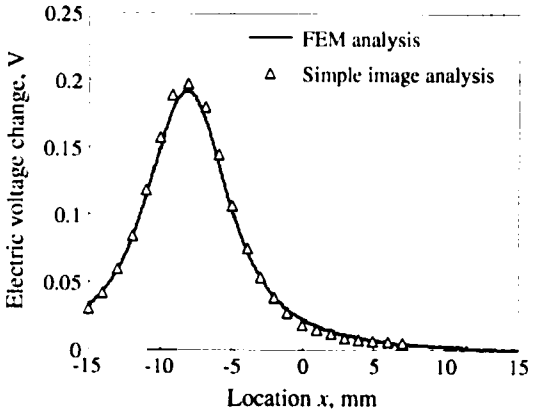

Figure 10. Electric voltage change calculated using the doublet distribution simple analysis method. (Delamination crack $z = 0.3$ [mm], $x_1 = -10$ [mm], $x_2 = -6$ [mm]).

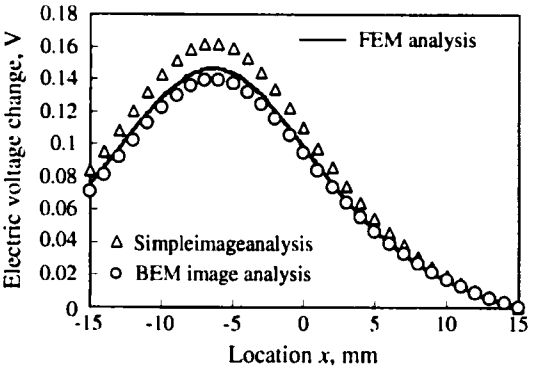

Figure 11. Comparisons of electric voltage changes calculated using doublet distribution BEM method and t he simple analysis method. (Delamination crack $z = 1.0$ [mm], $x_1 = -10$ [mm], $x_2 = -2$ [mm]).

of the boundary element method using singular elements with nine elements in total. As shown in Figure 11, both sets of analytical results show good agreement with the FEM results, although the simple method has small error. The value of small parallel shifts for the simple method must be considered in detail to obtain better results, which will form part of our future work.

4. Conclusions

The anisotropic electric potential function has been applied for a thin CFRP laminate using the image analysis method to calculate the electric voltage change caused by a delamination crack in the laminate. From the analysis of this potential function, an estimate of the required number of images was obtained. For the analysis of the delamination crack, the distributed double method that annihilates the electric current perpendicular to the crack was applied, and the results were compared with an FEM analysis. A summary of results obtained is as follows.

(1) For the thin CFRP laminate, electric current density can be exactly calculated using the anisotropic electric potential function with the image analysis method.
(2) The number of images required for an acceptable level of accuracy is formulated using the anisotropic electric potential function. Using the formula, the electric current of the thin CFRP laminate is calculated based on a practical number of images.
(3) To annihilate the electric current perpendicular to the delamination crack, the anisotropic electric potential of doublet is developed. The distributed anisotropic doublet can be obtained by solving a hyper-singular integral equation.
(4) Using the analysis of the anisotropic distributed doublet, the electric potential change of the CFRP surface caused by the existence of a delamination crack can be calculated simply.

References

[1] Schueler R, Joshi SP, Schulte K. Damage detection in CFRP by electrical conductivity mapping. Compos. Sci. & Tech. 2001;61–6:931–930.
[2] Louis M, Joshi SP, Brockmann W. An experimental investigation of though-thickness electrical resistivity of CFRP laminates. Compos. Sci. & Tech. 2001;61–6:911–919.
[3] Todoroki A, Tanaka M, Shimamura Y. Measurement of orthotropic electric conductance of CFRP laminates and analysis of the effect on delamination monitoring with electric resistance change method. Compos. Sci. & Tech. 2002;62:619–628.
[4] Hirano Y, Katsumata S, Iwahori Y, Todoroki A. Artificial lightning testing on graphite/epoxy composite laminate. Composites: Part A. 2010;41:1461–1470.
[5] Todoroki A. Electric current analysis of CFRP using perfect fluid potential flow. Trans. Japan Soc. Aero. Space Sci. 2012;55:183–190.
[6] Todoroki A. Electric current analysis for thick laminated CFRP composites. Trans. Japan Soc. Aero. Space Sci. 2012;55:237–243.
[7] Todoroki A, Tanaka Y. Delamination identification of cross-ply graphite/epoxy composite beams using electric resistance change method. Compos. Sci. & Tech. 2002;62:629–639.
[8] Katz J, Plotkin A. Low-speed aerodynamics second edition. Cambridge (UK): Cambridge University Press; 2001.
[9] Lifanov IK, Poltavskii LN, Vainikko GM. Hypersingular integral equations and their applications. Boca Raton (FL): Chapman & Hall/CRC; 2004.
[10] Arai M, Adachi T, Matsumoto H. Formulation of double-layer potential method. Trans. JSME, Ser. A. 1995;585:993–1000 [in Japanese].
[11] Arai M, Adachi T, Matsumoto H. Boundary element analysis for unsteady elastodynamic problems based on the laplace transform. JSME Int J., Ser. A. 1999;42:507–514.